Electronic Tuning Using Remote Substituents in Tetrakis(*μ*-*N*,*N*′-diarylformamidinato)dinickel. Linear Free Energy Relationships in Dinuclear Compounds. 3†

Chun Lin,‡ John D. Protasiewicz,§ and Tong Ren*,‡

Department of Chemistry, Florida Institute of Technology, Melbourne, Florida 32901, and Department of Chemistry, Case Western Reserve University, Cleveland, Ohio 44106

Received July 25, 1996

Introduction

The paddlewheel (or lantern) motif is very common for dinuclear transition metal compounds supported by three atom, bidentate bridging ligands, both with and without metal−metal bonds.[1,2] Although the catalytic properties of this class compounds are generally unexplored, a few have shown promise. For instance, dirhodium(II) carboxylates are among the best α-carbonylcarbene insertion catalysts,[3] diruthenium(II) carboxylates are efficient hydrogenation catalysts,[4] and the dicopper(II) complex of 7-azaindole catalyzes the regioselective oxygenation of benzyl ethyl ether.[5] We are particularly interested in how substituents away from the dinuclear core (remote substituents) affect both the molecular and electronic structures of the paddlewheel compounds, which in turn determine catalytic activity. Recently, we reported the first example of substituent electronic-tuning within a series of quadruply bonded dimolybdenum compounds supported by diarylformamidinate.[6] Some notable findings include that a linear correlation was established between the HOMO (δ(MoMo)) energy level and the Hammett constant of aryl-substituents, and minimum substituent influences were found in other parameters related to overall valence structure, such as the HOMO−LUMO gap and the composition of upper valence orbitals. The generality of these findings in paddlewheel compounds could be significant, since the frontier orbitals of a dinuclear catalyst may be tuned to yield a optimal match with that of a specific substrate while leaving other contributing factors unperturbed. A comprehensive probe of the above mentioned effects is being carried out with the systems of M−M bond orders other than four. Results from the series of tetrakis(*μ*-*N*,*N*′-diarylformamidinato)dinickel(II), a dinuclear species without a formal M−M bond, are presented here.

Results and Discussion

Compounds **1**−**9** (numbered according to the aryl substituent (X): **1** (*p*-OMe), **2** (*p*-Me), **3** (H), **4** (*m*-OMe), **5** (*p*-Cl), **6** (*m*-Cl), **7**, (*m*-CF_3), **8** (*p*-CF_3), and **9** (3,5-Cl_2)) were prepared as outlined in Scheme 1. These compounds can be synthesized by treating anhydrous $NiCl_2$ with excess lithiated formamidinate

Scheme 1

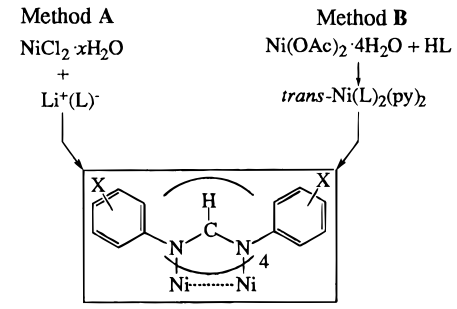

(method A), similar to the procedure for Ni_2[(*p*-tolyl)NCHN-(*p*-toly)]$_4$ (**2**) where $NiBr_2$ was used.[7] However, we could only achieve poor yield for purified samples (typically *ca.* 10−20%). An alternative route (method B) modified from that of dinickel triazenate was thus invoked,[8] where the mononuclear *trans*-Ni(η^2-*N*,*N*′-formamidinato)$_2$(py)$_2$ was generated first, and the subsequent pyrolysis of this compound led to the desired dinickel compound. Besides the significantly improved yield for purified samples (40−60%), method B also avoids necessitating anaerobic synthesis. Excellent agreement in ^{1}H NMR spectra was found between the compounds from method A and those from method B. Consistent with the early report,[7] ^{1}H NMR spectra of the purified samples revealed the presence of water (≥2 per complex), which was probably introduced during the recrystallization process.

A single-crystal X-ray diffraction study has provided both the overall topology and the metric parameters of **9**. A labeled ORTEP diagram is shown in Figure 1, where the paddlewheel framework is apparent. There exists a crystallographic 2-fold axis that is defined by C(1) and C(3) carbon atoms and relates one half of the molecule to the other. It was concluded in the previous study of **2** that there is no formal Ni−Ni bonding on the basis of the *d*-electron counting and the long Ni−Ni separation (2.485 Å).[7] The corresponding distance is 2.462(2) Å in **9**, and the contraction can be attributed to the partial removal of antibonding electron density due to the presence of strong electron-withdrawing group 3,5-Cl_2 (Hammett constant $\sigma_x = 0.74$). The averaged Ni−N distance in **9** (1.917[4] Å) is slightly increased from, but statistically the same as, that in **2** (1.904(5) Å),[7] indicating that the strength of Ni−N covalent bond is not significantly affected by varying the remote substituent. Interestingly, despite the increased steric bulkiness of the aryl group in **9**, the torsional angle N−Ni−Ni′−N′ (18.5°) is only increased slightly from that of **2** (16.8°). A much smaller torsional angle (9.5°) was found for tetrakis(*μ*-*N*,*N*′-di-*p*-tolylformamidinato)diruthenium(II) which has a metal−metal separation (2.474 Å) almost identical to that of **2** and **9**, but a higher bond order (Ru−Ru double bond).[9] Therefore, the large torsional angles observed for both dinickel and dipalladium[7] probably originate from the nonbonding nature of the dinuclear core, rather than the steric factors of bridging formamidinate.

The redox behavior of the dinickel compounds **1**−**9** has been examined by cyclic voltammetry, and the relevant parameters are listed in Table 1. Compounds **1**−**7** undergo a (quasi)-reversible one electron oxidation (Ni_2^{5+}/Ni_2^{4+}) and the corresponding $E_{1/2}$ (*vs* Ag/AgCl) ranges from 832 to 1492 mV. Compound **8** is redox inactive under the current experimental conditions, while compound **9** exhibits only an anodic peak at

† Part 2: Lin, C.; Protasiewicz, J. D.; Smith, E. T.; and Ren, T. *Inorg. Chem.* **1996**, *35*, 6422.

‡ Florida Institute of Technology.

§ Case Western Reserve University.

(1) Cotton, F. A.; Walton, R. A. *Multiple Bonds between Metal Atoms*, 2nd ed.; Oxford University Press: Oxford, England 1993.
(2) Umakoshi, K.; Sasaki, Y. *Adv. Inorg. Chem.* **1993**, *40*, 187.
(3) Doyle, M. P. In *Catalytic Asymmetric Synthesis*; Ojima, I., Ed.; VCH: New York, 1993.
(4) Lindsay, A. J.; McDermott, G.; Wilkinson, G. *Polyhedron* **1988**, *7*, 1239.
(5) Minakata, S.; Imai, E.; Ohshima, Y.; Inaki, K.; Ryu, I.; Komatsu, M.; Ohshiro, Y. *Chem. Lett.* **1996**, 19.
(6) (a) Lin, C.; Protasiewicz, J. D.; Smith, E. T.; Ren, T. *J. Chem. Soc., Chem. Commun.* **1995**, 2257; (b) Lin, C.; Protasiewicz, J. D.; Smith, E. T.; Ren, T. *Inorg. Chem*, in press.
(7) Cotton, F. A.; Matusz, M.; Poli, R.; Feng, X. *J. Am. Chem. Soc.* **1988**, *110*, 1144.
(8) Dwyer, F. P.; Mellor, D. P. *J. Am. Chem. Soc.* **1941**, *63*, 81.
(9) Cotton, F. A.; Ren, T. *Inorg. Chem.* **1991**, *30*, 3675.

S0020-1669(96)00842-7 CCC: $12.00

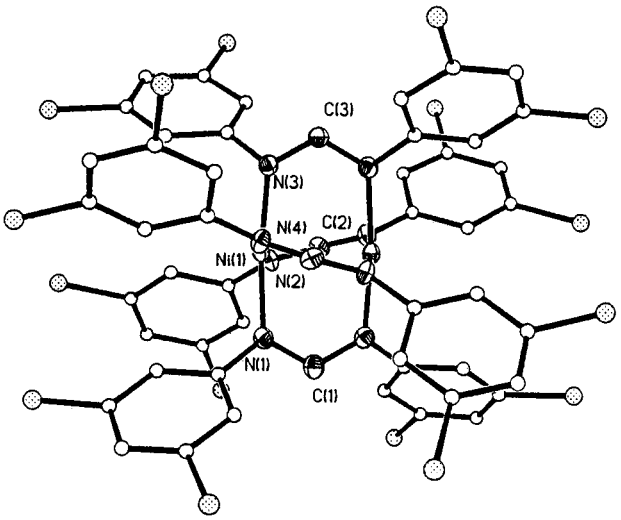

Figure 1. Structural diagram of compound **9**. Some averaged bond lengths (Å) and angles (deg) are as follows: Ni−Ni′ 2.4618(13), Ni−N 1.917[4], N−$C_{methine}$ 1.321[6]; Ni−Ni−N 86.7[1], *trans*-N−Ni−N 173.4[2], *cis*-N−Ni−N 89.8[2], N−$C_{methine}$−N 123.1[7], N−Ni−Ni′−N′ 18.5.

1727 mV. The gradual anodic-shift in $E_{1/2}$ upon increasing σ_x is similar to the trend observed for the dimolybdenum series.[6] It is apparent that the electron density residing on the N−C−N bridge decreases as the electron-withdrawing ability of the substituent increases, which in turn results in less electron density on the dinickel core and a more positive potential for the Ni_2^{5+}/Ni_2^{4+} couple. The remarkable range (900 mV between $E_{1/2}$(**1**) and $E_{p,a}$(**9**)) of redox potentials in the current series is among the largest for the metal-centered redox couples in a homologous series of coordination compounds. Other notable examples include the Cr^+/Cr^0 couple in (η^6-arene)$Cr(CO)_3$ (990 mV),[10] the Fe^{2+}/Fe^{1+} couple in the β-pyrrole cyano-substituted FeCl(tetraphenylporphyrin) complexes (780 mV),[11] and the Fe^{3+}/Fe^{2+} couple in the fully perhalogenated FeCl(tetraphenylporphyrin) complexes (600 mV).[12]

The quantification of redox tuning was achieved by correlating the $E_{1/2}$ with the Hammett constant of the substituents.[13] The Hammett equation derived from the linear least-squares fit (Figure 2, both compounds **8** and **9** were not included since their $E_{1/2}$s are unavailable) is given in eq 1, where ρ is the so-

$$\Delta E_{1/2} = E_{1/2}(\mathrm{X}) - E_{1/2}(\mathrm{H}) = \rho 8 \sigma_x \qquad \rho = 114 \text{ mV} \quad (1)$$

called reactivity constant, 8 is the number of substituents per complex, and the correlation coefficient (R) is 0.996. Since the oxidation corresponds to the removal of HOMO ($\sigma^*(Ni_2)$ or δ^*) electron,[7] the excellent linear correlation between $\Delta E_{1/2}$ and σ_x unambiguously attest that the HOMO energy level is precisely controlled by the remote substituent in the current series. The reactivity constant obtained for dinickel series ($\rho(Ni_2)$) is larger than that of dimolybdenum analogs (87.2 mV),[6] revealing that the Ni_2 core is more sensitive toward the substituent than the Mo_2 core. The increased sensitivity is likely due to the orbital origin of removed electrons: δ electron in Mo_2[6] and σ* or δ^* electron in Ni_2.[7] The reactivity constant for

Table 1. Experimental Results for $[Ni_2(ArNCHNAr)_4]$

	1 (*p*-OCH_3)	**2** (*p*-CH_3 [a])	**3** (−H)	**4** (*m*-OCH_3)	**5** (*p*-Cl)	**6** (*m*-Cl)	**7** (*m*-CF_3)	**8** (*p*-CF_3)	**9** (3,5-Cl_2)
σ	−0.27	−0.17	0	0.12	0.23	0.37	0.43	0.54	0.74
$E_{1/2}$ (mV)[b]	832 (157, 0.91)	904 (157, 0.64)	1048 (152, 0.61)	1175 (207, 0.54)	1265 (123, 0.86)	1371 (160, 0.70)	1492 (179, 0.77)		*c*
(ΔE_p (mV), i_{pc}/i_{pa})									
λ_{max} (nm)	298 (58200),	294 (69300),	288 (57000),	284 (38500),	294 (69000),	288 (63400),	290 (48200),	296 (51000),	292 (65600),
(ϵ (M^{-1} cm^{-1}))	394 (sh),	390 (sh),	384 (sh),	388 (sh),	394 (sh),	392 (sh),	390 (sh),	396 (sh),	400 (sh),
	478 (2430),	482 (2160),	478 (1810),	476 (1420),	478 (2410),	476 (2140),	474 (1800),	478 (1970),	474 (2470),
	632 (620)	632 (640)	630 (520)	630 (450)	630 (610)	630 (520)	630 (370)	634 (350)	630 (500)

[a] Spectroscopic and electrochemical data for this compound were reported in ref 7, but were redetermined here to ensure a consistent experimental condition across the series. Only minor deviation was noticed. [b] Measurement was carried out in CH_2Cl_2 with Bu_4NBF_4 as the supporting electrolyte, Pt working and auxiliary electrodes, Ag/AgCl reference electrode, [Ni_2] 1 mM, and scan rate 100 mV/s. Under these conditions, the $E_{1/2}(Fc^+/Fc)$ was consistently measured at +625 mV. [c] Irreversible oxidation.

(10) Hunter, A. D.; Mozol, V.; Tsai, S. D. *Organometallics* **1992**, *11*, 2251.
(11) Giraudeau, A.; Callot, H. J.; Jordan, J.; Ezhar, I.; Gross, M. *J. Am. Chem. Soc.* **1979**, *101*, 3857.
(12) (a) Bottomley, L. A.; Kadish, K. M. *Inorg. Chem.* **1981**, *20*, 1348. (b) Wijesekera, T.; Matsumoto, A.; Dolphin, D.; Lexa, D. *Angew. Chem., Int. Ed. Engl.* **1990**, *29*, 1028. (c) Grinstaff, M. W.; Hill, M. G.; Labinger, J. A.; Gray, H. B. *Science* **1994**, *264*, 1311.
(13) Zuman, P. *The Elucidation of Organic Electrode Processes*; Academic Press: New York, 1969.

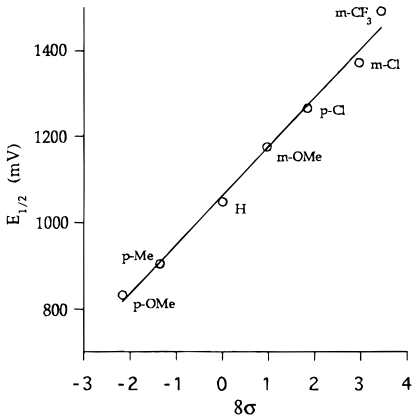

Figure 2. Hammett plot $E_{1/2}$ *vs* σ. The circles are the measured values, and the solid line is the least-squares fit. The datum for **2** was remeasured and included in the fit.

the oxidation of Ni(II) compounds is sensitive to the distance between substituted aryl and metal center: while a larger ρ is found for current series since the substituted phenyl is only two σ-bonds away from the Ni center, a value of 18 mV was determined for the Ni complexes of phenyl-substituted tetraphenylporphyrin (4 σ-bonds away),[14] and a range of 35−64 mV for the Ni complexes of benzoyl-derivatized tetraaza macrocyles (4 σ-bond away).[15]

Similar to the absorption spectra reported for **2**,[7] there are three well-resolved peaks and one shoulder observed for the series, a strong absorption ($\epsilon \sim 10^4$) around 290 nm, medium intensity absorptions ($\epsilon \sim 10^2-10^3$) around 480 nm and 630 nm, and the shoulder around 390 nm (see Table 1). Although the exact electronic origin of these absorptions could be neither resolved in the current study, nor deduced based on the Xα calculation of model compounds,[7] they are probably the metal to ligand charge transfer (MLCT) transitions from the occupied Ni-based antibonding orbitals to the empty π-antibonding orbitals of the N−C−N bridges. The unique feature about the electronic absorption spectra is that both the transition energies ($1/\lambda_{max}$) and the extinction coefficients are strikingly similar across the series, as can be seen from Table 1. Especially, the variance of λ_{max} is no more than 14 nm ($\leq$0.21 eV) for all four transitions, and apparently independent of the substituent. The "constant" absorption spectra clearly indicate that the *distribution* of energy levels of upper valence molecular orbitals, namely both the occupied Ni−Ni antibonding orbitals and the ligand-based low-energy virtual orbitals, is not influenced by the substituent. Therefore it is safe to conclude that while the HOMO orbital is energetically stabilized with the increasing electron withdrawing power (σ_x) of the substituent, so are the other nearby molecular orbitals, which yields a substituent-independent valence structure around the dinickel core.

Experimental Section

Formamidines were prepared and characterized as previously described.[6] $NiCl_2 \cdot 6H_2O$ (Fisher) was dehydrated at 160 °C under dynamic vacuum before use. $Ni(acetate)_2 \cdot 4H_2O$ was purchased from ACROS. THF was distilled over Na/benzophenone under N_2 before use and other solvents were dried over 4 Å molecular sieves. ^1H NMR spectra were recorded on a Bruker AMX-360 NMR spectrometer, with chemical shifts (δ) referenced to the solvent $CDCl_3$. UV−vis spectra were measured in CH_2Cl_2 with a Hewlett Packard 8452A diode array UV−vis spectrophotometer. Cyclic voltammograms were recorded with a BAS CV-50W voltammetric analyzer. Dinickel compounds were synthesized by either one or both of methods A and B which are described for X as *p*-OMe and *p*-Cl, respectively.

Method A. *N*,*N*′-Bis(*p*-methoxyphenyl)formamidine (1.13 g, 4.4 mmol) dissolved in 30 mL of THF was treated with 3.0 mL of 1.6 M *n*-BuLi (hexane) at −78 °C under argon. The lithium salt was transferred to a Schlenk flask containing $NiCl_2$ (0.258 g, 2.0 mmol) and the reaction mixture was refluxed under argon for 24 h. The mixture was filtered through a Celite column and the solid residue remained on the Celite was rinsed with CH_2Cl_2. The crude product obtained by removing the solvent from the combined filtrate was purified by column chromatography (silica) with CH_2Cl_2 as eluent. Evaporation of the solvent from the dark-brown elute yielded 0.125 g black polycrystalline **1** (11% based on $NiCl_2$).

Method B. To a hot pyridine solution of $Ni(OAc)_2 \cdot 4H_2O$ (0.249 g, 1.0 mmol) was added a solution of *N*,*N*′-bis(*p*-chlorophenyl)formamidine (0.530 g, 2.0 mmol) in pyridine. KOH in MeOH (1.5 mL, 2 N) was added dropwise while the mixture was heated at 90 °C. Greenish yellow precipitate formed immediately and the mixture was stirred at 90 °C for 2 h. Removal of the solvents via vacuum distillation yielded a light green residue, which was heated at 120 °C for 20 h under dynamic vacuum. The dark brown residue was extracted with benzene (2 × 20 mL). The crude product was precipitated from the extract with addition of hexanes, and recrystallized from benzene to yield 0.342 g (58%) of brown crystalline **5**.

UV−vis absorption data are listed in Table 1 and ^1H NMR data (δ (ppm)) are given below: **1**, 7.12 (d, 16 H), 6.76 (d, 16H), 6.15 (s, 4H, methine), 3.79 (s, 24H); **2**, 7.23 (d, 16H), 7.01 (d, 16H), 6.17 (s, 4H, methine), 2.28 (s, 24H); **3**, 7.33 (d, 16H), 7.21 (t, 16H), 7.07 (t, 8H), 6.28 (s, 4H, methine); **4**, 7.25, (s, 8H), 7.04 (t, 8H), 6.64 (m, 16H), 6.31 (s, 4H, methine); **5**, 7.22 (d, 16H), 7.15 (d, 16H), 6.22 (s, 4H, methine); **6**, 7.36 (s, 8H), 7.20 (m, 24H), 6.33 (s, 4H, methine); **7**, 7.73 (s, 8H), 7.38 (m, 24H), 6.45 (s, 4H, methine); **8**, 7.50 (d, 16H), 7.38 (d, 16H), 6.48 (s, 4H, methine); **9**, 7.35 (d, 16H), 7.24 (t, 8H), 6.41 (s, 4H, methine).

Crystallographic Analysis. Single crystals of **9** were grown by slow diffusion of hexanes into a benzene solution of **9**. A prismatic dark brown crystal (0.16 mm × 0.20 mm × 0.46 mm) was selected and mounted on a Siemens P4 diffractometer. The procedures for data collection, and structural solution and refinement are the same as previously described.[6] Crystal data and details of data collection and structure solution are summarized in Table 2.

Table 2. Crystal Data for **9**·2*n*-hexane

formula	$C_{64}H_{56}Cl_{16}N_8Ni_2$
fw	1621.79
cryst syst	monoclinic
space group	*C*2/*c*
a, Å	15.376(2)
b, Å	23.478(3)
c, Å	21.587(2)
β, deg	110.25(1)
V, Å^3	7311.5(13)
Z	4
ρ_{calc}, g cm^{-3}	1.473
μ, mm^{-1}	1.144
λ, Å	0.710 73
θ range, deg	2.01−24.00
T, °C	20(2)
R1[a]	0.0626
wR2[b]	0.1240
goodness-of-fit on F^2 [c]	1.190

[a] $R1 = \sum||F_o| - |F_c||/\sum|F_o|$. [b] $wR2 = [\sum[w(F_o^2 - Fc^2)^2]/\sum[w(F_o^2)^2]]^{1/2}$. [c] Goodness-of-fit $= [\sum[w(F_o^2 - F_c^2)^2]/(n-p)]^{1/2}$.

Acknowledgment. This work is partially supported by grants from Florida Solar Energy Center (to T.R.) and Department of Chemistry, Case Western Reserve University (to J.D.P.). The NMR facility at Florida Institute of Technology is supported

(14) (a) Kadish, K. M.; Morrison, M. M. *Inorg. Chem.* **1976**, *15*, 980. (b) Kadish, K. M.; Morrison, M. M. *J. Am. Chem. Soc.* **1976**, *98*, 3326. (c) Walker, F. A.; Beroiz, D.; Kadish, K. M. *J. Am. Chem. Soc.* **1976**, *98*, 3484.

(15) Streeky, J. A.; Pillsbury, D. G.; Busch, D. H. *Inorg. Chem.* **1980**, *19*, 3148.

through an NSF grant (CHE-9013145). Acknowledgment is also extended to Professor E. T. Smith for making the electrochemical apparatus available.

Supporting Information Available: Tables of spectroscopic data (^{13}C NMR and IR) for compounds **1** to **9** (Table S1); positional parameters for all atoms, bond lengths and angles, anisotropic temperature factors, and hydrogen atom parameters for compound **9** (Tables S2−S5) and a fully labeled ORTEP of diagram **9** (Figure S1) (7 pages). Ordering information is given on any current masthead page.

IC960842S